Theoretical and Experimental Effects of Spatial Dispersion on the Optical Properties of Crystals

J. J. HOPFIELD*†
Department of Physics, University of California, Berkeley, California

AND

D. G. THOMAS
Bell Telephone Laboratories, Murray Hill, New Jersey

(Received 14 June 1963)

The classical dielectric theory of optical properties is a local theory, and results in a dielectric constant dependent only on frequency. This dielectric behavior can be written as a sum over resonances, each resonance occurring at a particular frequency. The spatial dispersion (i.e., nonlocal dielectric behavior) effect considered here is the effect of the wave-vector dependence of the resonant frequencies on optical properties. The additional boundary condition needed for the application of such a theory is discussed for the case in which the resonance is due to an exciton band and the wave-vector dependence to the finite exciton mass. Experimental data presented on the reflection peaks due to excitons in CdS and ZnTe exhibit gross departures from the reflectivities expected from classical theory. Particularly striking are *sharp* subsidiary reflectivity spikes. The departures from classical results are all well represented by calculations based on the theory of spatial resonance dispersion and a simple approximation to the derived boundary condition.

I. INTRODUCTION

THE well-known classical optics of nonmagnetic crystals is based upon the concept of local dielectric behavior. In this approximation, the dielectric polarization $\mathbf{P}$ within a small volume of radius r_0 ($r_0 \ll$ any wavelength involved) depends only on the value of the electric field inside this volume (at the present time and in the past) and is *not* explicitly dependent on the electric field or other parameters outside the volume under consideration.

The term "spatial dispersion" has been used to apply to dielectric behavior for which the local description is not valid. In general, spatial dispersion refers to the wave-vector dependence of the dielectric constant.

Implicitly contained in the supposition of local dielectric behavior is the neglect of the transport of energy by any mechanism other than electromagnetic waves. When energy transport by other mechanisms must be considered anomalous (nonlocal) dielectric behavior results, often accompanied by new physical phenomena. For example, a metal in which the electron mean free path becomes smaller than the classical skin depth exhibits the anomalous skin effect.[1] In this case, the energy transported by the electrons is, in the interior of the crystal, as important as the energy transported by the electromagnetic field.

Of all possible spatial dispersion effects, we confine ourselves to the one which seems to be the most radical in effect in classical optics, namely, the effect of a second mechanism of energy transport on classical optics. In particular, the effect of a noninfinite exciton mass on the reflectivity of insulating crystals near an isolated exciton line is investigated both theoretically (Secs. II and III) and experimentally (Sec. V). Section IV contains a brief account of general experimental and theoretical problems involved in demonstrating the effect of spatial dispersion in the exciton region.

II. THEORY

The development of the theory of spatial dispersion in optical spectra of excitons has in great part been due to Pekar[2,3] in a series of papers beginning in 1957. The nature of this theory has unfortunately been obscured by its formalism. In this section, the rudiments of the theory of spatial dispersion are developed from a simple classical point of view.

Let an electric field $\mathbf{E}_0 e^{i\mathbf{k}\cdot\mathbf{x}} e^{-i\omega t}$ exist in a crystal. A polarization wave

$$\mathbf{P} = \left(\sum_{\mathbf{G}} \boldsymbol{\alpha}(\mathbf{k}+2\pi\mathbf{G}, \omega) e^{2\pi i \mathbf{G}\cdot\mathbf{x}}\right) \mathbf{E}_0 e^{i\mathbf{k}\cdot\mathbf{x}} e^{-i\omega t}, \quad (1)$$

where $\mathbf{G}$ is a reciprocal lattice vector and $\boldsymbol{\alpha}(\mathbf{k}+2\pi\mathbf{G}, \omega)$ is a second-rank tensor function of $\mathbf{k}+2\pi\mathbf{G}$ and ω, will accompany the electric field. By restricting consideration to sufficiently low energies [$\omega \ll c/$(lattice constant)] the terms of nonzero $\mathbf{G}$ introduce only renormalization corrections which can be absorbed in $\boldsymbol{\alpha}(k,\omega)$. In this approximation,

$$\mathbf{P}_k(\omega) = \boldsymbol{\alpha}(k,\omega)\mathbf{E}_{\mathbf{k}}(\omega) \quad (2)$$

and $\boldsymbol{\alpha}(k,\omega)$ can be regarded as the frequency- and wave-vector-dependent polarizability tensor. It describes the polarization response in a "Gedanken" experiment for which k and ω are independently specified.

By "the effects of spatial dispersion" we mean the effect of the wave-vector dependence of α in (2). Classi-

* Alfred P. Sloan, Research Fellow.
† Supported in part by the National Science Foundation.
[1] G. E. H. Reuter and E. H. Sondheimer, Proc. Roy. Soc. (London) **A195**, 336 (1948).
[2] S. I. Pekar, Zh. Eksperim. i Teor. Fiz. **33**, 1022 (1957) [translation: Soviet Phys.—JETP **6**, 785 (1958)].
[3] S. I. Pekar, Fiz. Tverd. Tela **4**, 1301 (1962) [translation: Soviet Phys.—Solid State **4**, 953 (1962).]

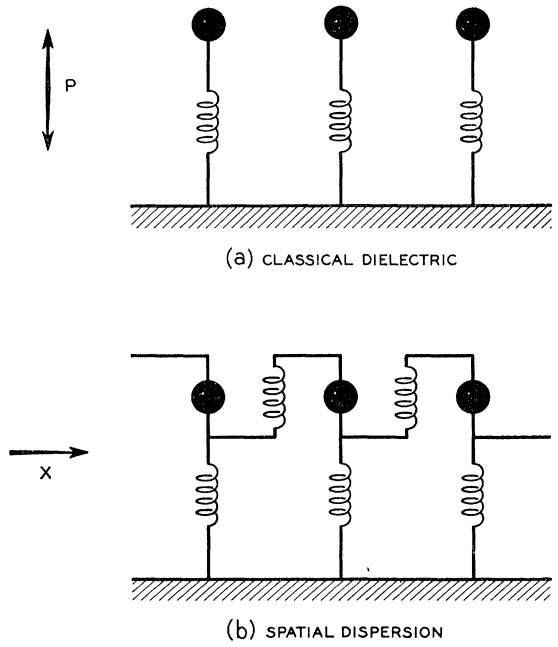

FIG. 1. The spring and charged mass-point models of a classical dielectric, (a); and one exhibiting spatial resonance dispersion, (b). These models represent scalar analogs to the actual vector equations. The directions of P and x are indicated.

cal local dielectric theory is obtained simply by setting $\mathbf{k}=0$ in (2).

For a given wave vector, insulating crystals are characterized by polarizabilities of the form

$$\boldsymbol{\alpha}(\mathbf{k},\omega)=\sum_j \frac{\boldsymbol{\alpha}_j(\mathbf{k})\omega_j^2(k)}{\omega_j^2(k)-\omega^2-i\omega\Gamma_j(\mathbf{k})}, \tag{3}$$

by virtue of the fact that the polarizability obeys a Kramers-Kronig relation at any fixed wave vector. [The summation in (3) should be understood to include the possibility of integration over the index j.] A conventional isolated optical absorption line is associated with an isolated resonance, a single term L for which $\omega_j(0)$ is isolated from the other zero wave-vector resonant frequencies.

The presence of resonances in (3) prevents $\boldsymbol{\alpha}(\mathbf{k},\omega)$ from being usefully expanded in powers of $\mathbf{k}$. Instead, both the numerator and denominator (of each term) must be expanded.

To keep the physics from disappearing in a morass of tensor notation, the problem will be simplified. First, the frequency will be chosen near a particular resonance in (3), and the sum over all other oscillators will be lumped into a frequency- and wave-vector-independent background dielectric constant ϵ. Second, the wave-vector dependence of the phenomenological damping term Γ will be ignored. (Indeed, the calculations of Sec. IV show that the value of Γ is small enough to be ignored in some experiments.) Third, a direction of $\mathbf{k}$ is chosen such that $\boldsymbol{\alpha}$ has one principal axis parallel to $\mathbf{k}$ and the others perpendicular to $\mathbf{k}$ in directions independent of the magnitude of $\mathbf{k}$ (e.g., $\mathbf{k}$ is in a $\langle 100\rangle$ direction in a cubic crystal). Fourth, only the zero and second-order terms in the expansion of $\alpha(k)$ and $\omega_j(k)$ will be retained. The first-order terms will vanish in a crystal having inversion symmetry and will be small under much broader circumstances. For $\mathbf{E}$ polarized in a given principal direction, (2) is approximated by

$$P_k(\omega)=\left[\frac{\epsilon_0-1}{4\pi}+\frac{(\alpha_0+\alpha_2k^2)\omega_0^2}{\omega_0^2+Bk^2-\omega^2-i\omega\Gamma}\right]E_k(\omega). \tag{4}$$

The solutions (periodic in space and time) to Maxwell's equations for the dielectric defined by (2) are found by solving the eigenvalue problem,

$$k^2\mathbf{E}_\mathbf{k}-\mathbf{k}(\mathbf{E}_\mathbf{k}\cdot\mathbf{k})=\left(\frac{\omega^2}{c^2}\right)\mathbf{D}_\mathbf{k}\equiv\frac{\omega^2}{c^2}[\mathbf{E}_\mathbf{k}+4\pi\mathbf{P}_\mathbf{k}]. \tag{5}$$

Under the approximations described, the solutions of (5) divide themselves into longitudinal solutions ($\mathbf{E}_\mathbf{k}$ parallel to $\mathbf{k}$) and transverse solutions.

When (4) is substituted into (5), the transverse solutions to (5) are determined by the condition

$$n^2\equiv\frac{c^2k^2}{\omega^2}=\epsilon_0+\frac{4\pi(\alpha_0+\alpha_2k^2)\omega_0^2}{\omega_0^2+Bk^2-\omega^2-i\omega\Gamma}. \tag{6}$$

For real frequencies, k and n will be in general complex.

In classical optics, $\alpha_2=B=0$. For a given frequency, (6) is linear in k^2, and there are two roots for k. These roots are the complex numbers, k and $-k$ one referring to a right-running and one to a left-running solution. For a given (principal) polarization, frequency, and direction of propagation only one transverse mode exists. The case $B=0$, $\alpha_2\neq 0$ is rather similar to the classical case. Although there will be some effects of the wave-vector dependence (in particular, when $\alpha_0=0$, a "forbidden" absorption line will be seen if $\alpha_2\neq 0$, a line which would be absent in classical optics), (6) remains linear

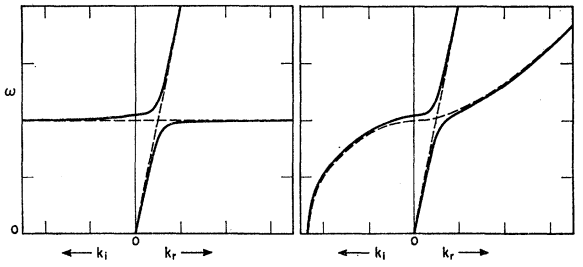

FIG. 2. The frequency wave-vector dispersion relation for the transverse normal modes of light coupled to a classical dielectric (graph at left) and a dielectric having spatial resonance dispersion (at right). No damping is included. The normal mode wave vectors are in either case either purely real or purely imaginary, and are plotted to the right or left accordingly. The dashed lines show the dispersion relations for $\alpha_0=$zero; the solid lines for a finite α_0. Parameters have been chosen to display clearly the differences between the models.

in k^2, and no profound change of the electromagnetic equations results.

The case $B\neq 0$, $\alpha_2=0$ is much more interesting. For this case, given ω, (6) is quadratic in k^2. There are in this case *two* transverse solutions propagating in *each* direction for a given principal polarization and frequency.

That there should be two propagating modes is easily seen by examining a mechanical model of a classical dielectric, and comparing it to a model which exhibits a nonvanishing B. The model of Fig. 1(a), in a continuous limit, defines a classical dielectric. Figure 1(b) defines a dielectric with $B\neq 0$. The transverse normal modes for the two systems are shown in Fig. 2. The equations of motion for the local oscillator polarization $P_{ex}(x)$ in the continuous limit (but without damping) are of the form

$$\frac{1}{\omega_0^2}\frac{\partial^2 P_{ex}(x)}{\partial t^2}+P_{ex}(x)=\alpha_0 E(x), \tag{7a}$$

$$\frac{1}{\omega_0^2}\frac{\partial^2 P_{ex}(x)}{\partial t^2}+P_{ex}(x)-B\frac{\partial^2 P_{ex}}{\partial x^2}=\alpha_0 E(x), \tag{7b}$$

for the two cases, respectively, for transverse waves propagating in the x direction. If $E(x)$ and $P(x)$ have the forms $E_k \exp[i(k_x-\omega t)]$ and $P_{ex,k}\exp[i(k_x-\omega t)]$, then the exciton contribution to the polarizability $P_{ex\ k}/E_k$ determined from (7b) is the second term on the right in (6) for the case $\alpha_2=\Gamma=0$.

When springs between the polarization oscillators are included there are, even for $\alpha=0$, two methods of propagating energy at a given frequency, one "electromagnetic" and one "mechanical." The coupling due to α, of course, mixes the modes, but does not change their number.

The wave-vector dependence of the denominator in (6) has an obvious interpretation. The normal mode of the crystal to which the light couples clearly has the dispersion relation,

$$\omega^2=\omega_0^2+Bk^2 \quad \text{or} \quad \hbar\omega\approx h\omega_0+\frac{1}{2}\frac{\hbar^2k^2}{m^*}. \tag{8}$$

For the case of a dielectric resonance due to an exciton band, m^* is by definition of the exciton mass.

The rest of the present paper concerns, of all spatial dispersion effects, only those effects due to the noninfinite "mass" (nonzero B). To distinguish these effects from more general ones, we shall refer to them as being due to "spatial resonance dispersion."

III. BOUNDARY CONDITIONS

We consider here the effect of the wave-vector dependence of the energy of an isolated pole of the dielectric constant on the optical reflectivity of a crystal. Only the simplest case experimentally attainable is treated, normal incidence in a principal direction. For normal incidence, all wave vectors involved in the problem are collinear. To appreciate the importance of the choice of a principal direction, it must be recalled that a finite α_0 in (4) requires an "oscillator" having vector properties. In a cubic crystal at $\mathbf{k}=0$, such an oscillator is degenerate, transforming like x, y, z. Away from $\mathbf{k}=0$, the degeneracy splits. In a $\langle 100\rangle$ or $\langle 111\rangle$ direction, the form of the degenerate perturbation theory splitting is determined from symmetry considerations. The splitting in these directions is into purely longitudinal and purely transverse modes. At normal incidence in a principal direction, a single transverse polarization can be chosen, the longitudinal mode does not enter, and the resultant wave equation and boundary value problem are one dimensional and scalar.

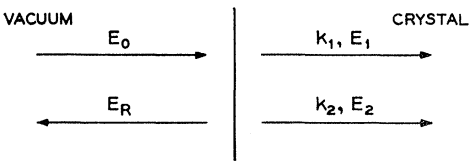

FIG. 3. A schematic diagram of the normal incidence reflectivity problem. The arrows denote the wave directions, and the different E's the wave electric field amplitudes.

The model dielectric under consideration has a dielectric constant

$$\epsilon(k,\omega)=\epsilon_0+\frac{4\pi\alpha_0\omega_0^2}{\omega_0^2-\omega^2+(\hbar k^2\omega_0/m^*)-i\omega\Gamma}, \tag{9}$$

in a frequency region near ω_0. (This dielectric constant applies to a case in which the exciton polarization and the electric field are parallel, and both perpendicular to $\mathbf{k}$. In a uniaxial crystal, the electric field must, in addition, be either parallel or perpendicular to the optic axis.) The wave-vector dependence of ϵ_0 is neglected (Sec. II).

The reflectivity boundary problem to be solved is illustrated in Fig. 3. Unlike the classical problem, there are two right-running waves in the medium. The usual Maxwell boundary conditions on E, B, D, and H must, of course, be satisfied. These conditions become

$$\begin{aligned} E_0+E_R&=E_1+E_2,\\ E_0-E_R&=n_1E_1+n_2E_2, \end{aligned} \tag{10}$$

where $n_1=ck_1/\omega$, $n_2=ck_2/\omega$, and k_1 and k_2 are the two "right-running" roots of the dispersion relation $c^2k^2/\omega^2=\epsilon(k,\omega)$. Substituting (9) into (5) [equivalent to (6)], n_1^2 and n_2^2 are found to be given by

$$\begin{aligned} n^2=\frac{1}{2}\Big[\epsilon_0-\Big(1-\frac{\omega^2}{\omega_0^2}-i\frac{\Gamma\omega}{\omega_0^2}\Big)\frac{(mc^2)\omega_0}{\hbar\omega^2}\Big]\\ \pm\Big\{\frac{1}{4}\Big[\epsilon_0+\Big(1-\frac{\omega^2}{\omega_0^2}-i\frac{\Gamma\omega}{\omega_0^2}\Big)\frac{mc^2\omega_0}{\hbar\omega^2}\Big]^2\\ +4\pi\alpha_0\frac{mc^2\omega_0}{\hbar\omega^2}\Big\}^{1/2}. \end{aligned} \tag{11}$$

For the classical case of *one* mode of propagation in the medium, (10) can be solved for the reflection coefficient E_R/E_0. In the case of two modes of propagation, these equations are not sufficient to determine a solution; an additional boundary condition is needed.

This need of an additional boundary condition is evident in comparing the dielectric models of Fig. 1 and Eq. (7). In the continuum limit, the differential equation of motion of P is of zero order in x for Fig. 1(a), but second order for Fig. 1(b). For the second-order equation, a boundary condition on P at the termination of the medium is needed (just as at the end of a continuous elastic bar). This boundary condition is specified by the manner of termination in the case of an elastic medium (e.g., a bar with a free end has the boundary condition that the strain vanish at the end).

The oscillators by which the dielectric polarization P can be described are abstract. The problem is to find the appropriate boundary condition for these oscillators. The optical excitation of direct excitons results in discrete exciton absorption lines due to isolated oscillators. The boundary condition on P_{ex}, the contribution of a single exciton mode to the dielectric polarization, will be investigated for one of these transitions.

Several previous investigations of boundary conditions[3-5] have been made, yielding three different boundary conditions. One of these (Ref. 4) is incorrect. The difficulty with the other two is that each is appropriate to a model which does not contain sufficient generality to apply to the real physical world.

The exciton as a quantum-mechanical particle can be specified by its internal state and its total wave vector k. Given a particular internal state, the eigenvalue equation for the exciton is

$$E(k)\psi(k)=E\psi(k), \tag{12}$$

where $E(k)$ is the exciton band energy. For a given direction of k, $E(k)$ is expandable in powers of k. Expanding around the minimum of $E(k)$ (presumed at $k=0$) and considering only waves propagating in the x direction, the free exciton effective-mass equation [valid for $|(E-E_0)/E_0|\ll 1$]

$$\left(-\frac{h^2}{2m^*}\frac{\partial^2}{\partial x^2}+E_0\right)\psi(x)=E\psi(x),$$
$$E(k)\approx E_0+\frac{h^2k^2}{2m}, \tag{13}$$

is obtained as the Fourier transform of (12).

If a (perfect) crystal exists only for $x>0$, a free exciton incident from the right will be totally reflected back to the right by the crystal boundary. The exciton wave function, for $x>0$ but well away from the boundary, must then have the form

$$\psi(x)\propto e^{ikx}+e^{-i\varphi}e^{-ikx}, \tag{14}$$

where φ is a real function of the energy.

To calculate φ, a microscopic understanding of the forces which cause the exciton to turn around is necessary. The investigation of these forces in the *absence* of a coupling between the light and excitons for two idealized cases follows.

A. Frenkel Excitons with Nearest-Neighbor Interactions

For the one-dimensional problem under consideration, represent the crystal by a line of equivalent atoms, each of which has a single excitation state and coupling to its nearest neighbors. The linearized exciton Hamiltonian, in terms of the operators $b_i^+(b_i)$ which excite (de-excite) atom i is

$$H=\sum_{i=0}^{\infty}[Ab_i^+b_i-J(b_{i+1}^+b_i+b_i^+b_{i+1})]. \tag{15}$$

If the sum extended also to all $i<0$, the crystal would fill all space and plane-wave states would be eigenstates. For the truncated crystal, the normal mode creation operators are of the form

$$\sum_{j\geqq 0}[e^{ik(x_j+a)}-e^{-ik(x_j+a)}]b_j^+, \tag{16}$$

where a is the lattice constant, and have, of course, the plane-wave exciton energy

$$E_k=A-2J\cos ka. \tag{17}$$

The exciton "wave function" as a function of position is, from (16),

$$\psi(x_i)=e^{ik(x_j+a)}-e^{-ik(x_j+a)}, \tag{18}$$

and defined only at lattice points. In the exciton effective mass approximation, x_j can be replaced by a continuous function $\psi(x)$. All the normal modes of the semi-infinite lattice obey the "boundary condition" $\psi(x)=0$ when extended outside the crystal to the point $x=-a$. For long wavelengths, the boundary condition is approximately

$$\psi(0)\approx a(\partial\psi/\partial x)(0), \tag{19}$$

or, more crudely,

$$\psi(0)\approx 0. \tag{20}$$

Equation (20) is the boundary condition calculated by Pekar.[3]

It is, of course, possible to add other terms to (15) to terminate the crystal. For example, A could be modified for atom zero. Such a modification still leads to a boundary condition of the general form of (19) for small k, with a multiplied by a numerical factor.

[4] V. L. Ginzburg, Zh. Eksperim. i Teor. Fiz. **34**, 1593 (1958) [translation: Soviet Phys.—JETP **7**, 1096 (1958)].

[5] J. J. Hopfield, Ph.D. thesis, Cornell University, 1958 (unpublished).

This case is seldom literally applicable, but demonstrates clearly the origin of the exciton boundary condition.

B. The Case of Wannier-Mott Excitons

Consider a simple hydrogenic exciton in its ground ($1S$) state. The interaction between the exciton and its image charge results in a potential energy of the exciton

$$V(x)=-\frac{1}{2}\left(\frac{\epsilon-1}{\epsilon+1}\right)E_B\left(\frac{a}{x}\right)^3, \tag{21}$$

where a is the exciton Bohr radius, E_B the exciton binding energy, and ϵ the static dielectric constant. Since ϵ is greater than 1, the force is repulsive. Shorter range effects of "overlap" with the surface, surface field, etc., also contribute to the effective potential.

If all the effects of the surface could be represented by a potential $U(x)$ for the exciton, $U(x)$ would have to be sufficiently repulsive to cause the exciton to be totally internally reflected. In such a case, the exciton Schrödinger equation and boundary condition

$$-\frac{h^2}{2m^*}\frac{\partial^2\psi}{\partial x^2}+h\omega_0\psi(x)+U(x)\psi(x)=h\omega\psi(x), \tag{22}$$
$$\psi(x)=0, \quad x\leq 0,$$

completely specify the reflection of the exciton at the surface. For $|E-E_0|\ll E_B$, the classical turning point is well removed from $x=0$. In this energy region, the energy region of real interest, the potential is characterized by exciton parameters, and is independent of detailed knowledge of the crystal surface.

An exciton is the "particle" of the classical polarization field in the same sense that the photon is the particle of quantum electrodynamics. The exciton wave function $\psi(x)$ is in reality a boson field operator. The operator $P_{ex}(x)$ which gives the exciton contribution to the polarization field is proportional to $\psi(x)+\psi^*(x)$. Replacing ω by $i(\partial/\partial t)$ in (22), the equations of motion of P_{ex} in the absence of an electric field for frequencies $|(\omega-\omega_0)/\omega_0|\ll 1$, is given by (23).

$$\left[\frac{\partial^2}{\partial t^2}+\omega_0^2-\frac{h\omega_0}{m^*}\frac{\partial^2}{\partial x^2}+2\frac{\omega_0 U(x)}{h}\right]P_{ex}(x,t)=0 \tag{23}$$
$$=\alpha_0\omega_0^2E(x,t). \tag{24}$$

The presence of an electric field simply adds a term $\alpha\omega_0^2E(x,t)$ as in (24), to lowest order. Semiclassical radiation theory is now recovered by reinterpreting the P and E operators in (24) as classical fields.

Two simple cases emerge. First, for $m^*\to\infty$, the left-hand side of (24) expresses the classical polarizability of a medium whose resonant frequency changes near the surface. Second, for $U(x)=0$, the polarizability determined by (24) is that represented by the second term on the right in (9) if damping is neglected.

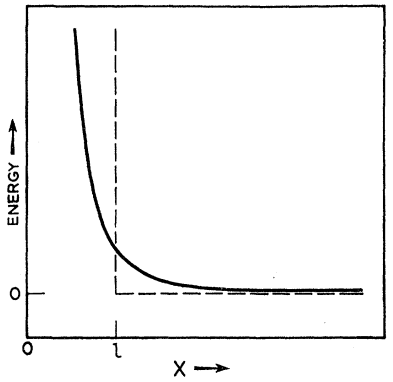

FIG. 4. Energy versus x for the potential $U(x)$ (solid line) and the infinite barrier approximation (dashed line).

The boundary condition problem can now be adequately described. For case A, $U(x)=0$. Approximate boundary condition (20) implies $P_{ex}(0)=0$. If this is the case, the two propagating modes must sum to no exciton polarization at $x=0$, and the additional boundary condition is therefore

$$P_{ex_1}+P_{ex_2}=0 \quad \text{or} \quad (n_1^2-\epsilon_0)E_1+(n_2^2-\epsilon_0)E_2=0. \tag{25}$$

A slightly more complicated boundary condition can be derived for boundary condition (19).

For case B, $U(x)$ is not equal to zero, and a much more complicated equation must be solved, namely,

$$x<0: \quad \frac{\partial^2E}{\partial x^2}=+\frac{1}{c^2}\frac{\partial^2E}{\partial t^2},$$
$$x>0: \quad \frac{\partial^2E}{\partial x^2}=\frac{1}{c^2}\frac{\partial^2}{\partial t^2}(\epsilon_0E+4\pi P_{ex}), \tag{26}$$

Equation (24),

subject to the boundary conditions

$$E(0_-)=E(0_+),$$
$$\frac{\partial E}{\partial x}(0_-)=\frac{\partial E}{\partial x}(0_+), \tag{27}$$
$$P_{ex}=0, \quad x\leq 0,$$

and the asymptotic conditions best described by looking at Fig. 3. The solution is then determined since $U(x)$ is sufficiently singular to eliminate the exciton P_{ex} at the boundary.

The solution of (26) and (27) is annoyingly difficult. The chief physical effect of the repulsive $U(x)$ is to cause the free exciton to be totally reflected from an effective barrier a finite distance inside the surface. One is tempted, therefore, to replace the potential $U(x)$ by an infinite potential barrier a finite distance l inside the crystal as indicated in Fig. 4. At and to the left of such

a barrier, the boundary condition $P(l)=0$ will apply. In this case, there will be three spatial regions, $x<0$, $0<x<l$, and $x>l$. The first two are characterized by classical indices of refraction 1 and $\sqrt{\epsilon_0}$, respectively. The third region is anomalous. The usual Maxwell boundary conditions plus the $P_{ex}=0$ boundary conditions determine the connection between the second and third regions.

The l which best represents (27) is not clear. A guess might be the l for which the energy in (22) is the same as the exciton-phonon interaction energy $2\pi\alpha_0\hbar\omega_0/\epsilon_0$. This yields the estimate that l is about twice the exciton Bohr radius for all semiconductors.

The reflection coefficient $R=E_R/E_0$ can now be calculated. It is conveniently written

$$R=(1-n^*)/(1+n^*), \tag{28}$$

where n^* is an effective index of refraction. For the case A with boundary condition (20),

$$n^\dagger=(n_1n_2+\epsilon_0)/(n_1+n_2), \quad n^*=n^\dagger. \tag{29}$$

Case B, with the repulsive barrier approximation, has the reflectivity the same as it would be for a classical dielectric interface having three layers of $n=1$, $\sqrt{\epsilon_0}$, and $n^\dagger$, respectively. One finds for this case $n^\dagger$ is given by (29), but n^* for (28) is given by

$$n^*=n\left[\frac{(n^\dagger+n)e^{-2ikn l}-n+n^\dagger}{(n^\dagger+n)e^{-2ikn l}+n-n^\dagger}\right]. \tag{30}$$

IV. INTERPRETATIONAL PROBLEMS

Several attempts have been made[6–8] to observe the effect of spatial resonance dispersion on optical properties near exciton absorption peaks. One of the striking properties of spatial resonance dispersion is the predicted existence of additional propagating waves in a crystal. The interference between the two propagating waves (when classical optics would have produced but one wave) should, in principle, produce observable effects on the optical transmission. If all multiple reflection effects are neglected (and all classical interference effects therefore impossible in isotropic materials for normal incidence on a plane parallel slab), two kinds of oscillatory effects should be observed. One is a periodic modulation of the transmission at fixed energy as a function of the thickness. The other is a periodic modulation of the transmission at fixed thickness as a function of the energy due to the variation of the two indices of refraction with energy. These effects are attractive ones to investigate, since their existence can be theoretically predicted independently of the precise boundary condition employed.

This mode of experiment suffers from one chief defect. In order to obtain an interference effect, it is necessary for both modes of propagation to traverse the crystal and to arrive at the back with finite amplitude. In order to obtain this, it is necessary that the collision time of a bare exciton be comparable to or greater than the exciton transit time for the crystal used. For typical semiconductors, the characteristic velocity of the excitons involved is about 10^6 cm/sec. [This velocity is no greater than $2\pi\hbar/\lambda_{vac}m_{ex}$ or $((4\pi\alpha_0/\epsilon_0)(\hbar\omega_0)m_{ex})^{1/2}$, whichever is greater.] Since characteristics relaxation times (collision times) are of the order of 10^{-11}–10^{-13} sec, crystals having thicknesses of the order of 10–1000 Å are necessary.

The experiments performed on Cu_2O by Gorban and Timofeev[6] in which an interference effect as a function of thickness is reported cannot, we believe, be viewed as a verification of the theory. The oberved linewidth gives in this case an exciton collision time of about 10^{-12} sec, whereas the transit time in crystals of the thickness used ($\sim$100 000 Å) is of the order of 10^{-4} sec. In addition, the data show no oscillations at fixed thickness. It seems likely that the observed results are an artifact of the indirect method of measurement.

The experiments of Brodin and Pekar[7] are much more likely to demonstrate the interference effects. The thickness of crystal investigated was of a more appropriate thickness 500–3000 Å. Unfortunately, there is not sufficient data on anthracene to make an independent estimate of either the mean free path or the exciton mass. The oscillation periods are different at the two frequencies reported.

Recent experiments by Brodin and Strashnikova[8] have shown that the dispersive and absorptive parts of the index of refraction of CdS (as obtained from a classical analysis of thin film measurements) do not appear to be quantitatively compatible. They have suggested that the cause of this incompatibility is spatial dispersion.

The incompatibility with classical analysis seems quite plausible. Any effect which changes the boundary conditions in an energy-dependent fashion (as spatial dispersion does) will automatically introduce inconsistencies, even if only one mode crosses the crystal. To confirm this hypothesis, quantitative calculations would be necessary.

Reflectivity experiments have one real advantage over other varieties of experiments for detection of spatial resonance dispersion, namely that thin crystals are not needed. For crystals several absorption lengths thick, the results are independent of thickness. Further, the reflectivity results are expected in theory to be independent of the exciton collision time as long as this time is sufficiently large. (This domain of $\tau\approx10^{-11}$ sec can be experimentally attained by the careful selection

[6] I. S. Gorban' and V. B. Timofeev, Doklady Akad. Nauk S.S.S.R. **140**, 791 (1961) [translation: Soviet Phys.—Doklady **6**, 878 (1962)].

[7] M. S. Brodin and S. I. Pekar, Zh. Eksperim. i Teor. Fiz. **38**, 74 (1960); **38**, 1910 (1960) [translations: Soviet Phys.—JETP **11**, 55 (1960); **11**, 1373 (1960)].

[8] M. S. Brodin and M. I. Strashnikova, Fiz. Tverd. Tela **4**, 2454 (1962) [translation: Soviet Phys.—Solid State **4**, 1798 (1963)].

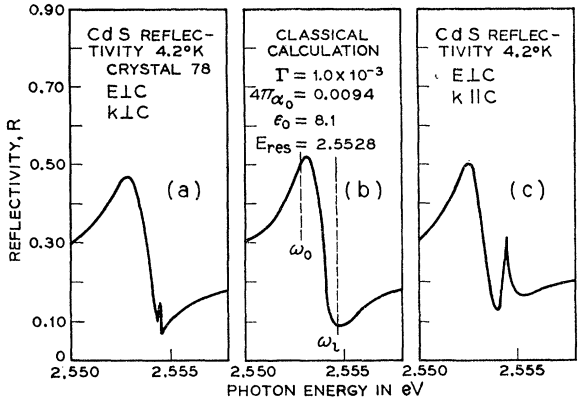

FIG. 5. The normal incidence reflectivity spectrum of CdS in the vicinity of the first exciton peak for two different but classically equivalent geometries [(a) and (c)]. A classical reflectivity curve crudely representing these anomalies is shown in (b).

of CdS crystals. The absence of an $n=2$ state in the dispersion curves of Brodin and Strashnikova[8] suggests that their τ was an order of magnitude shorter.)

Reflectivity experiments also have their drawbacks, the chief of which is the question of what the surface looks like. Experimental reproducibility defines a surface condition, but it is not necessarily the condition used, of a perfect crystal-vacuum interface, assumed for the theory.

In addition, the theoretical expression for the reflectivity is algebraically so complicated that one loses all intuition concerning the expected form of the reflectivity. Armed with the knowledge that, in order to compute quantitatively experimental results in any spatial resonance dispersion experiment on excitons, an understanding of the boundary condition at an actual surface is necessary, we proceed.

V. EXPERIMENTAL OBSERVATIONS AND CALCULATIONS

All experimental reflectivity spectra described here were taken on "good" CdS and ZnTe crystals at 1.6–4.2°K. The spectra were measured using a Bausch and Lomb grating spectrograph with a linear dispersion of 2 Å/mm. Some spectra were obtained from a photographic plate, but the more detailed spectra in CdS were measured photoelectrically. In some experiments, great care was taken to keep the cone of incidence and angle of incidence as small as 2°. No observable difference between these experiments and experiments using angles of incidences 2–3 times larger was observed. It is therefore believed that no qualitative (and only small quantitative) differences exist between these experiments and ideal ones performed with parallel light at normal incidence. "Good" crystals of CdS was taken to mean crystals in which the higher states of the excitons from the first valence band were observable in reflection. In really good crystals, the $n=3$ state is observable as an anomaly in the reflection, and the $n=2$ state shows a very marked and unusual reflection peak (see Fig. 9). The good crystals also showed the sharpest structure for the reflectivity of the $n=1$ state. Experiments were performed both on ZnTe (cubic) and ZnTe with a uniaxial strain. Under the uniaxial stress, the degenerate valence band splits and becomes simple, while the optical properties become uniaxial.

Reflection was always observed from as-grown faces with the crystals immersed in liquid helium. CdS grown from the vapor occurs as plates with the hexagonal c axis in the plane of the plates. Reflection measurements with $\mathbf{k}\perp c$ therefore presented no problems. For $k\|c$ crystal were found which had grown faces perpendicular to the c axis. These faces had a width of only 10–20 μ so that an enlarged image of the face was arranged to fall on the spectrograph slit. The ZnTe crystals were grown from the vapor,[9] and were stressed in an apparatus similar to one already described.[10]

Reflectivities were normalized by using a reflectivity calculated from the index of refraction in a spectral region where the crystal is transparent.

The reflectivity spectrum of CdS in the vicinity of the lowest exciton (exciton A) at 4.2°K is given in Fig. 5(a) for light at normal incidence in a direction perpendicular to the c axis and also polarized perpendicular to the c axis. The reflectivity of a classical oscillator (width 10^{-3} eV, $4\pi\alpha_0=0.0094$, $\epsilon_0=8.1$) is shown in Fig. 5(b). The two are rather similar, the difference being chiefly the small reflectivity peak at 2.55445 eV (marked by the arrow) not present in 5(b), and a quantitative failure to agree at energies at and slightly above the reflectivity minimum.

Two quandaries present themselves. First, the width of the classical dispersion oscillator which qualitatively fits the reflectivity is about 10^{-3} eV, whereas the width of the exciton state involved, as inferred from transmission experiments performed in other geometries, must be less than 10^{-4} eV. Second, there occurs near the reflectivity minimum a sharp peak not anticipated by the simple classical form 5(b). It would be tempting to explain the order of magnitude disagreement of the reflectivity linewidth and the transmission linewidth by assuming that the crystal is not as good, and the lines are broader at the surface (where the reflection is determined), rather than deep in the interior. This supposition is not really compatible with the observed sharpness of the subsidiary structure, nor does it explain this structure.

Exciton "A" in CdS is twofold degenerate, polarized in the plane perpendicular to the c axis. For wave vector perpendicular to the c axis ($\mathbf{k}\perp\mathbf{c}$), "$A$" splits into a longitudinal and a transverse exciton, at frequencies ω_l and ω_0, respectively. The zero of the index of refraction (of a transverse mode of propagation) occurs at energy

[9] R. T. Lynch, D. G. Thomas, and R. E. Dietz, J. Appl. Phys. 34, 706 (1963).

[10] D. G. Thomas, J. Appl. Phys. 32, 2298 (1961).

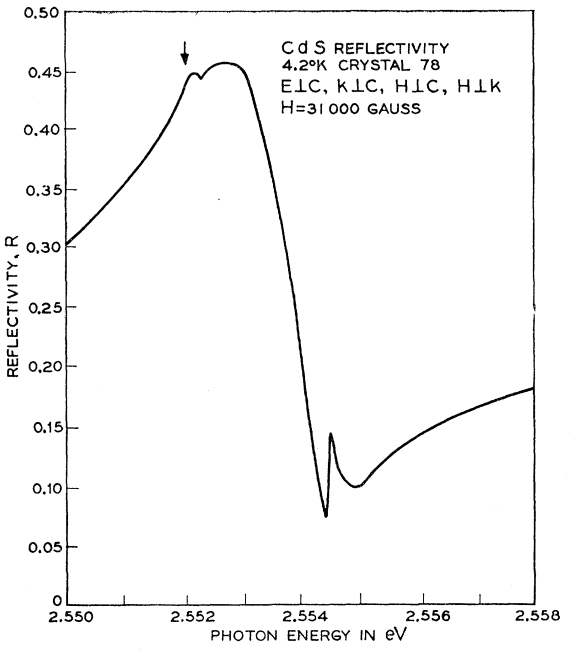

FIG. 6. The normal incidence reflectivity spectrum of Fig. 5(a) in the presence of a magnetic field. Additional structure introduced by the field is indicated by the arrow.

$\hbar\omega_l$. This energy is, within experimental error, the energy at which the sharp additional reflectivity structure occurs. The longitudinal energy is known from previous transmission experiments.[11]

The reflectivity measurement in CdS was repeated with $\mathbf{E}\perp\mathbf{c}$, at normal incidence, the only change being that the wave vector (and the normal to the reflecting surface) was parallel to the c axis. The results are shown in Fig. 5(c). The extra peak at the longitudinal frequency is much enhanced, and the form of the reflectivity at energies above this peak is much flatter than that in 5(b) or 5(a). Since, in this geometry, both components of exciton A are transverse but the subsidiary peak at the longitudinal frequency is very pronounced, the peak is presumably due to the zero of the index of refraction, not to the longitudinal exciton. Of particular note is the fact that 5(a) and 5(c) should be the same in classical theory, (except for the possibility of surfaces not representative of the bulk material).

Additional experiments have been done which demonstrate the sharpness of the exciton states seen in reflection. For example, Fig. 6 shows the normal incidence reflectivity measured with $\mathbf{k}\perp\mathbf{c}$, $\mathbf{E}\perp\mathbf{c}$, with a magnetic field of 31 000 G in the same direction as $\mathbf{E}$. An exciton state A_F, lying about 0.0013 eV below A_T[11] (an energy difference caused by electron-hole spin-spin interactions), and normally not seen in reflectivity, gains an admixture of A_T in this magnetic field. This line can be seen in reflection, and is marked by the arrow. It occurs as a clearly visible singularity characteristic of a classical oscillator of a width of about 10^{-4} eV, and having an oscillator strength of about 2% of the main peak. Similar experiments have been carried out in two other geometries, with similar results: When weak additional reflection singularities are introduced (by a magnetic field), they are characteristic of narrow exciton states.

Various models. of surface regions on classical dielectrics have been attempted to explain the apparent contradiction in linewidth and the subsidiary reflectivity maximum. Since any transparent (nonlossy) surface layer will lead to a total reflection region (for vanishingly small loss in the bulk material) in classical theory, it is necessary to postulate that the reflectivity is dominated by a lossy surface region in order to keep the reflectivity maximum down to a value of 50%. No model with such a region was consistent with the experiments in a magnetic field, and no model not containing additional *ad hoc* energies produced appropriate additional peaks.

If one rejects an attempt at purely classical interpretation and uses instead formulas applicable to spatial resonance dispersion, some of the quandaries are made plausible. Since an undamped exciton of positive mass, in the presence of spatial resonance dispersion, always has a propagating mode, the reflectivity without damping is never 100%. Reflectivities of less than 100% in the classical total reflection region are therefore not directly indicative of linewidth, and one large stumbling block to the understanding of the experiments is removed. Because there are rapid changes in $n^\dagger$ and n^* near the longitudinal frequency, this is the logical place for any peculiarities to occur. Strange effects can now be

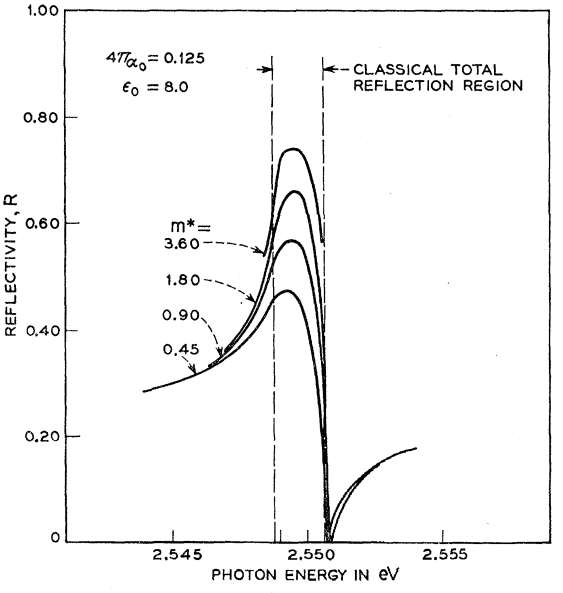

FIG. 7. The calculated reflectivity taking spatial dispersion into account (but without damping) for the case $l=0$ as a function of the exciton effective mass (in units of the free electron mass). For an infinite exciton mass, the classical result of total reflection would occur between the indicated limits.

[11] J. J. Hopfield and D. G. Thomas, Phys. Rev. **122**, 35 (1961).

introduced by a transparent (lossless) surface region. Mathematically necessary to these effects is a real part of $n^{\dagger}$, and such a real part is introduced by spatial dispersion. Finally, the exciton effective mass for exciton A is 0.9 m_e for $\mathbf{k}\perp\mathbf{c}$ [Fig. 5(a)] and about 3–5 times larger for $\mathbf{k}\|\mathbf{c}$ [Fig. 5(c)]. A natural reason for a difference between 5(a) and 5(c) is therefore present in spatial resonance dispersion.

Figure 7 shows the effect of spatial resonance dispersion without a surface barrier ($l=0$) [Eqs. (28) and (29)]. The ϵ_0 and $4\pi\alpha_0$ chosen here are the same as in Fig. 5(a). [A phenomenological damping term can be added to the denominator of (9), but has no noticeable effects on Fig. 7 for widths less than 10^{-4} eV. Figure 7 contains no damping.] The finite mass has, in these cases, an effect on the reflectivity maximum rather like an increased damping. The main reflectivity peaks 5(a) and 5(c) do *not* therefore necessitate the supposition of a width an order of magnitude too large.

Figure 8 shows the effect of a surface barrier (finite l) on the calculated reflectivity. The exciton mass used was 0.9 m_0.[11] A subsidiary sharp reflectivity peak is introduced, which falls within 10^{-4} eV of the $\mathbf{k}=0$ longitudinal optical frequency. The general behavior of the reflectivity both above and below this peak is also modified. It is clear that the experimental results of Fig. 5 can be well understood in terms of the effect of spatial dispersion with a surface barrier, if the effective surface barrier thickness l is dependent upon the exciton mass. As the Bohr radius of the 1S exciton in CdS is about 27 Å, the effective barrier thickness is, as anticipated, a few Bohr radii.

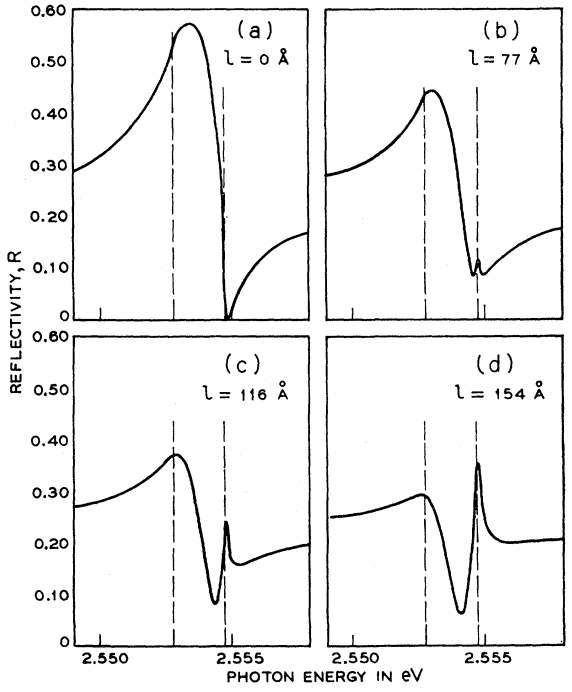

FIG. 8. The calculated reflectivity taking spatial dispersion into account as a function of l. The other parameters used are $m^*=0.9$, $4\pi\alpha_0=0.125$, and $\epsilon_0=8.0$. The longitudinal and transverse exciton energies at $k=0$ (the classical total reflection limits) are indicated by the vertical dashed lines.

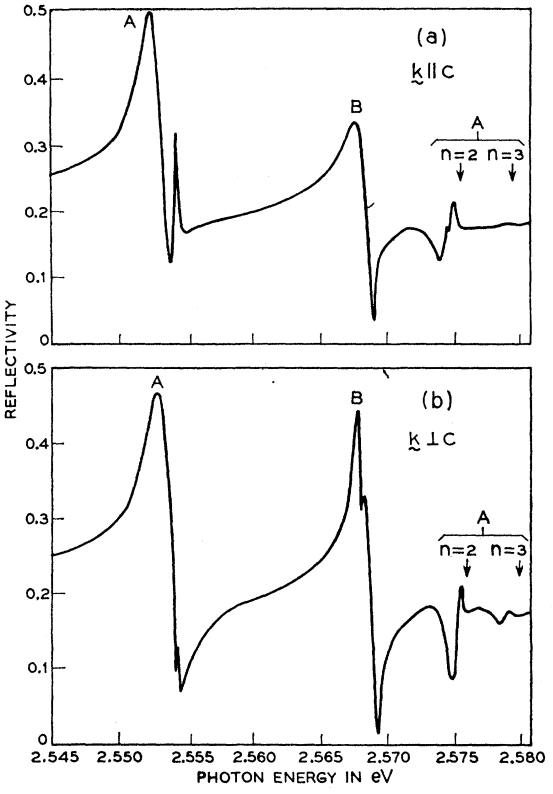

FIG. 9. The reflection curves for exciton A in a "good" crystal (59P) of CdS at 1.6°K. (a) refers to $\mathbf{k}\|\mathbf{c}$, (b) to $\mathbf{k}\perp\mathbf{c}$. The position of the $n=2$ and 3 states of exciton A have been marked. The large peak marked B is the $n=1$ state of exciton B. Notice the differences for these two classically equivalent geometries (both have $\mathbf{E}\perp\mathbf{c}$), and the unusual shapes of the reflection anomalies.

This reflectivity peak is not the only one in CdS which has a nonclassical form. Indeed, every reflectivity peak seen in CdS for $\mathbf{E}\perp\mathbf{c}$ has a bizarre shape, and shows differences between the classically equivalent geometries for $\mathbf{k}\|\mathbf{c}$ and $\mathbf{k}\perp\mathbf{c}$. We have chosen to analyze exciton "A" because of the knowledge of the masses, the clarity of the experimental effect, and the fact that this exciton state is the one in CdS most legitimately treated as "isolated." It also presumably has the longest τ. The experimentally observed reflection curves of exciton A for $\mathbf{k}\perp\mathbf{c}$ and $\mathbf{k}\|\mathbf{c}$, for "good" crystals, showing the $n=1$, 2, and 3 reflection anomalies are shown in Fig. 9.

Lest the reader receive the impression that the experiments and calculations are unique to CdS, experimental measurements and calculations of reflectivities for an exciton peak in ZnTe are shown in Fig. 10. In order to avoid the theoretical complications possible due to a degenerate valence band, the experimental results shown are for a crystal stressed in a ⟨111⟩ direction,

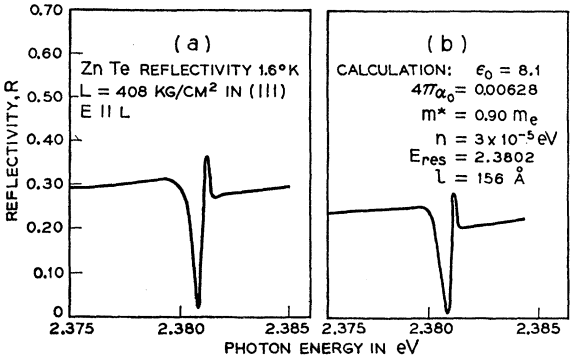

FIG. 10. (a) The measured normal incidence reflectivity spectrum of stressed ZnTe for light polarized parallel to the direction of stress. (b) A calculated reflectivity curve including spatial dispersion, using the parameters indicated.

using light polarized parallel to this direction. (In fact, the experimental reflectivity in this geometry is virtually unaffected by the strain except for a slight energy shift.) No effort was made to accurately fit the experimental reflectivity with the calculation; the object was simply to show the qualitative agreement. The two very similar curves bear no resemblance to the usual classical reflectivity. The usual classical rise approaching the resonant frequency is almost completely suppressed, and the spike at the longitudinal frequency becomes the reflectivity maximum.

The origin of the sharp reflectivity structure at the longitudinal frequency has no obvious physical meaning, but can be seen mathematically. In the absence of damping, one of the indices of refraction in Eq. (29) (let us say n_1) behaves, near the longitudinal frequency ω_l, as

$$n_1 \propto (\omega-\omega_l)^{1/2}$$

[see Eq. (11)]. Thus, the real part of n^+ has a vertical tangent just above ω_l, while the imaginary part has a vertical tangent immediately below ω_l. The same is true of n^*. The expression for the reflectivity $|R|^2$ therefore has the approximate form

$$|R|^2 \approx \frac{[1-n_l-A(\omega-\omega_l)^{1/2}]^2+k_l^2}{[1+n_l+A(\omega-\omega_l)^{1/2}]^2+k_l^2}, \quad (\omega>\omega_l)$$

$$|R|^2 \approx \frac{(1-n_l)^2+[k_l+A(\omega_l-\omega)^{1/2}]^2}{(1+n_l)^2+[k_l+A(\omega_l-\omega)^{1/2}]^2}, \quad (\omega<\omega_l)$$

where n_l and k_l and A are slowly varying real functions of frequency. If A is positive, $n_l<1$, and k_l negative, a sharp peak is produced very near ω_l.

Damping will quickly round off the singularity of n_1. It is not surprising that the spike has nearly vanished in CdS when the temperature is raised to 20°K. When the damping of the exciton becomes sufficiently large (comparable to the longitudinal-transverse energy splitting) the effects of spatial dispersion on optical properties disappear. The surface potential will not, however, disappear and will continue to have an influence on properties such as the reflectivity. The effect of damping limits the possible observation of spatial resonance dispersion effects to relatively strong absorption lines.

VI. CONCLUSION

The present paper has presented an array of experimental reflectivity measurements which have not proved amenable to any classical interpretation. The common features of the observed anomalies are that exciton states which are known to be narrow show unexpectedly low peak reflectivities, that the reflectivity minimum occurs at too low an energy, that a sharp additional reflection maximum occurs very near the longitudinal exciton energy, and the reflectivity is larger and less rapidly varying than expected at energies slightly above the longitudinal energy. These features are all predicted for reflectivity taking spatial resonance dispersion into account using a new boundary condition.

The new boundary condition is based upon the existence of a strong repulsive potential for the exciton near the surface of a crystal. The calculations including spatial resonance dispersion were made using an idealized model of the effect of such a potential. The agreement between the experiment and the calculations is sufficiently striking that one has confidence in the general physics of the boundary condition. In order to completely justify the model and to make interesting experimental use of the effects, the theory of excitons in the surface region must be completed by actually solving the Eqs. (26) and (27).

This complication of the reflectivity spectrum does not reduce the utility of ellipsometric and Kramers-Kronig determinations of optical parameters near sharp excitons dispersion peaks. It must, however, be born in mind that such measurements are related to effective optical parameters only, and have only an indirect theoretical connection to the parameters related to optical transmission. (For example, the effective absorption constant determined from the Kramers-Kronig relation and the reflectivity can have either sign.)

Since band gaps, exciton oscillator strengths, exciton masses, and exciton radii are the same (within factors of 2) for most II–VI compounds, the effects of spatial resonance dispersion will certainly be observable in the reflection spectrum of most II–VI compounds and probably in many other materials also. Although the present study was restricted theoretically to very simple exciton bands, and experimentally, chiefly to uniaxial crystals, more complicated systems should be tractable in simple geometries.

ACKNOWLEDGMENTS

The authors would like to thank G. D. Mahan, University of California, for his assistance with the calculations.